

## Electronic Supplementary Information

### Chemoselective oxidative addition of vinyl sulfones mediated by Palladium complexes bearing picolyl-*N*-heterocyclic carbene ligands.

Thomas Scattolin<sup>a</sup>, Claudio Santo<sup>b</sup>, Nicola Demitri<sup>c</sup>, Luciano Canovese<sup>b</sup> and Fabiano Visentin<sup>b,\*</sup>.

<sup>a</sup> Department of Chemistry and Center for Sustainable Chemistry, Ghent University, Krijgslaan 281 (S-3), 9000, Ghent, Belgium.

<sup>b</sup> Dipartimento di Scienze Molecolari e Nanosistemi, Università Ca' Foscari, Campus Scientifico Via Torino 155, 30174 Venezia-Mestre, Italy. E-mail: [fvise@unive.it](mailto:fvise@unive.it).

<sup>c</sup> Elettra – Sincrotrone Trieste, S.S. 14 Km 163.5 in Area Science Park, 34149 Basovizza, Trieste, Italy.

#### CONTENTS

- Fig. S1a: <sup>1</sup>H NMR spectrum of complex **2a** in CD<sub>2</sub>Cl<sub>2</sub> at 298 K
- Fig. S1b: <sup>13</sup>C {<sup>1</sup>H} NMR spectrum of complex **3a** in CD<sub>2</sub>Cl<sub>2</sub> at 298 K
- Fig. S1c: Selected part of the HMQC spectrum of the complex **1a** in CD<sub>2</sub>Cl<sub>2</sub> at 233 K
- Fig. S2a: <sup>1</sup>H NMR spectrum of complex **1b** in CD<sub>2</sub>Cl<sub>2</sub> at 233 K
- Fig. S2b: NOE interactions (up) and selected part of the NOESY spectrum of the complex **1b** in CD<sub>2</sub>Cl<sub>2</sub> at 233 K (down)
- Fig. S3a: <sup>1</sup>H NMR spectra of complex **1c** in CDCl<sub>3</sub>, recorded at 298 K and at 328 K. At this last temperature the spectrum remains unaltered even after 24 hours. The broadening of some signals is ascribable to dynamic processes activated at high temperature (ring inversion of chelating ligand).
- Fig. S3b: <sup>1</sup>H NMR spectra of complex **1c** in CD<sub>3</sub>CN, recorded at 298 K and at 333 K. At this last temperature the spectrum remains unaltered even after 24 hours. The broadening of some signals is ascribable to dynamic processes activated at high temperature (ring inversion of chelating ligand).
- Fig. S3c: <sup>1</sup>H NMR spectra of complex **1c** in dmsO-d<sub>6</sub>, recorded at 298 K and at 353 K. At this last temperature the spectrum remains unaltered even after 24 hours. The broadening of some signals is ascribable to dynamic processes activated at high temperature (ring inversion of chelating ligand).

- Fig. S3d:  $^1\text{H}$  NMR spectra of complex **1c** in  $\text{CD}_3\text{OD}$ , recorded at 298 K and at 333 K. At this last temperature the spectrum remains unaltered even after 24 hours. The broadening of some signals is ascribable to dynamic processes activated at high temperature (ring inversion of chelating ligand)
- Fig. S3e:  $^1\text{H}$  NMR spectra of final mixture of **2a/2c** in  $\text{CDCl}_3$ , recorded at 298 K and 328 K. At this last temperature the solution was kept for 24h without changing its composition.
- Fig. S4a:  $^{13}\text{C}$   $\{^1\text{H}\}$  NMR spectrum of complex **1c** in  $\text{CD}_2\text{Cl}_2$  at 298 K
- Fig. S4b: Selected part of the HSQC spectrum of the complex **1c** recorded at 233 K in  $\text{CD}_2\text{Cl}_2$  identifying the vinyl carbons
- Fig. S4c: NOE interactions (up) and selected part of the NOESY spectrum of the complex **1c** in  $\text{CD}_2\text{Cl}_2$  at 233 K (down)
- Fig. S5: Graphic representation of the DFT computational output.
- Table S1. Crystallographic data.
- Table S2. Selected palladium coordination spheres distances and angles ( $\text{\AA}$  and degrees) for **2c** (grey sticks) and the bromo[3-(2,6-diisopropylphenyl)-1-( $\alpha$ -lutidyl)imidazol-2-ylidene]methyl-palladium(II) complex CCDC 194155.
- Fig. S6. Ortep representation of complex **2c** (ellipsoids dimensions correspond to 50% probability). Atom labels in use are reported.
- Fig. S7. Stick representation of **2c** showing the angle of  $75.67(5)^\circ$  between the Pd coordination plane and the vinyl ligand.
- Fig. S8. Stick representation of **2c** (grey sticks) overlapped to CCDC 194155 (yellow sticks), showing the equivalent conformations adopted by the 1-( $\alpha$ -picolyl)imidazol-2-ylidene ligand (R.M.S.D. =  $0.10 \text{ \AA}$ ).
- Fig. S9:  $^1\text{H}$  NMR spectrum of complex **1a** in  $\text{CDCl}_3$  at 298 K
- Fig. S10:  $^{13}\text{C}$   $\{^1\text{H}\}$  NMR spectrum of complex **1a** in  $\text{CDCl}_3$  at 298 K
- Fig. S11:  $^{13}\text{C}$   $\{^1\text{H}\}$  NMR spectrum of complex **1b** in  $\text{CD}_2\text{Cl}_2$  at 233 K
- Fig. S12:  $^{13}\text{C}$   $\{^1\text{H}\}$  NMR spectrum of complex **2a** in  $\text{CD}_2\text{Cl}_2$  at 298 K
- Fig. S13:  $^{13}\text{C}$   $\{^1\text{H}\}$  NMR spectrum of final mixture of **2a/2c** in  $\text{CDCl}_3$  at 298 K
- Fig. S14:  $^1\text{H}$  NMR spectrum of complex **3a** in  $\text{CDCl}_3$  at 298 K
- Fig. S15:  $^1\text{H}$  NMR spectrum of final mixture of **3a/3c** in  $\text{CD}_2\text{Cl}_2$  at 298 K
- Fig. S16:  $^{13}\text{C}$   $\{^1\text{H}\}$  NMR spectrum of final mixture of **3a/3c** in  $\text{CD}_2\text{Cl}_2$  at 298 K

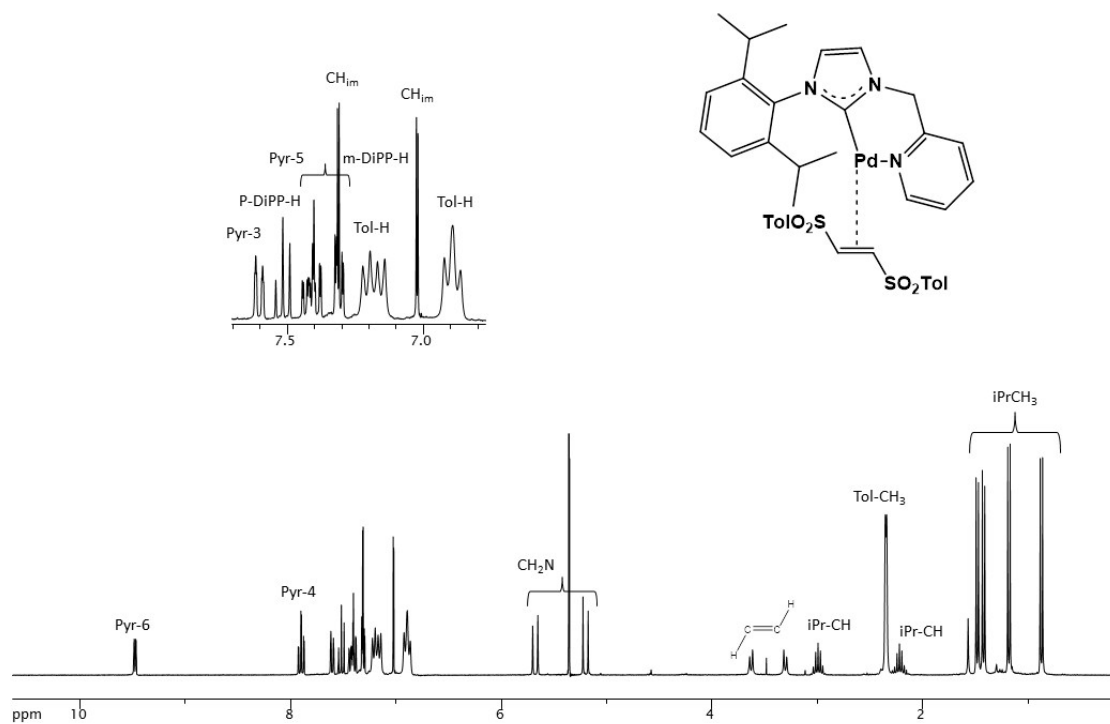


**Fig. S1a:**  $^1\text{H}$  NMR spectrum of complex **2a** in  $\text{CD}_2\text{Cl}_2$  at 298 K

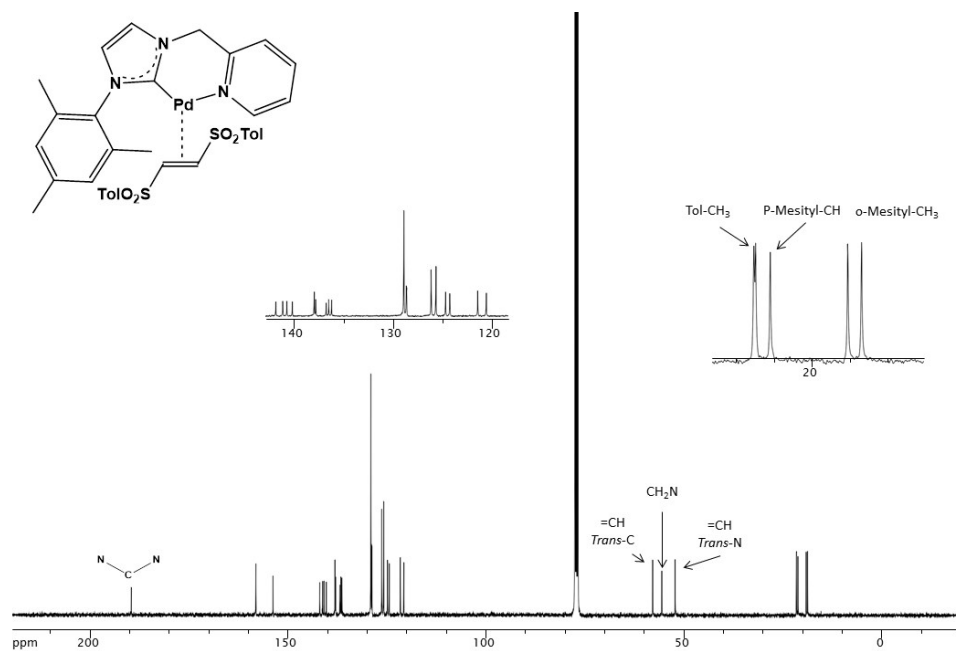


**Fig. S1b:**  $^{13}\text{C}$   $\{^1\text{H}\}$  NMR spectrum of complex **3a** in  $\text{CD}_2\text{Cl}_2$  at 298 K

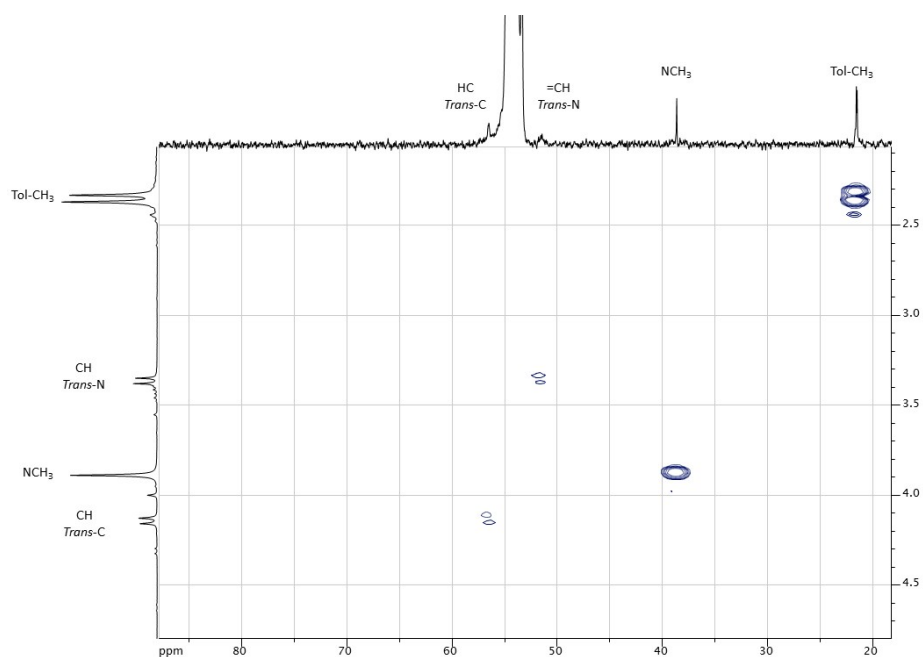


**Fig. S1c:** Selected part of the HMQC spectrum of the complex **1a** in  $\text{CD}_2\text{Cl}_2$  at 233 K

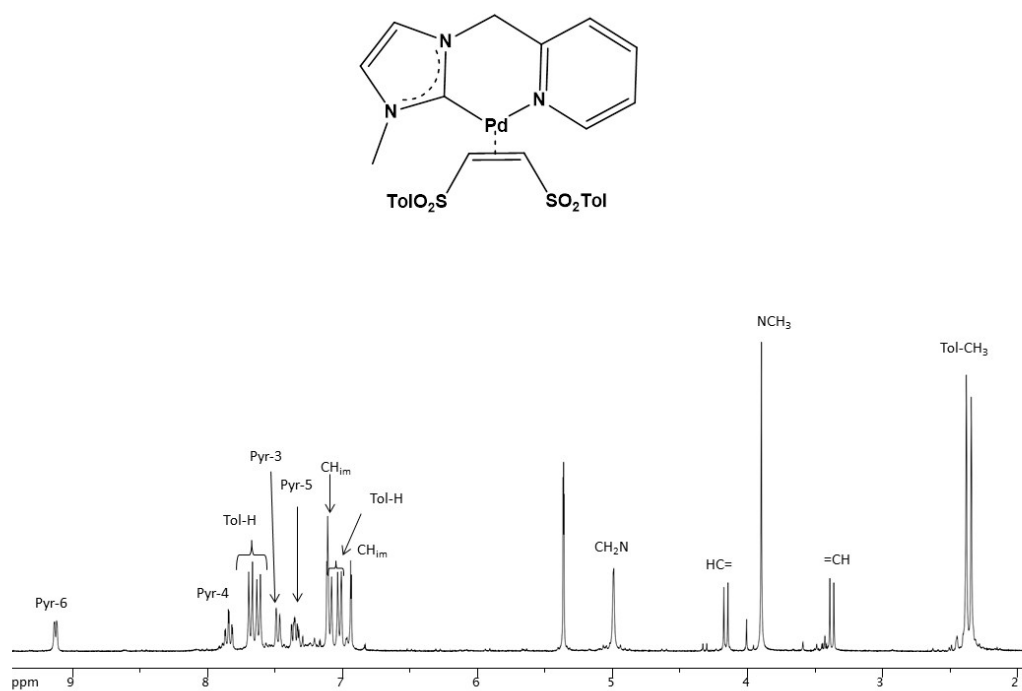


**Fig. S2a:**  $^1\text{H}$  NMR spectrum of complex **1b** in  $\text{CD}_2\text{Cl}_2$  at 233 K

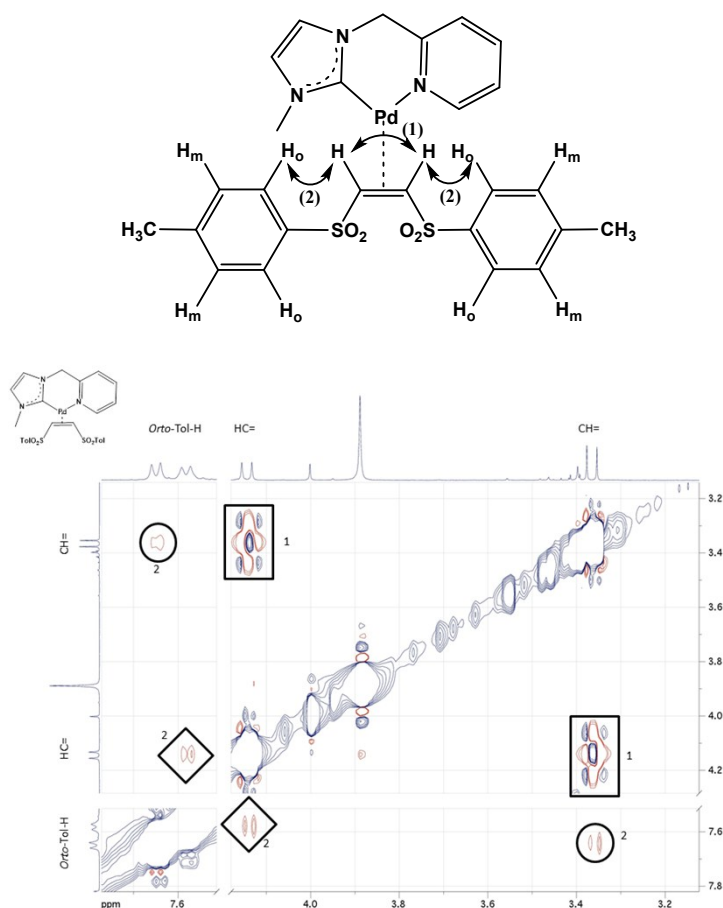


**Fig. S2b:** NOE interactions (up) and selected part of the NOESY spectrum of the complex **1b** in  $\text{CD}_2\text{Cl}_2$  at 233 K (down)

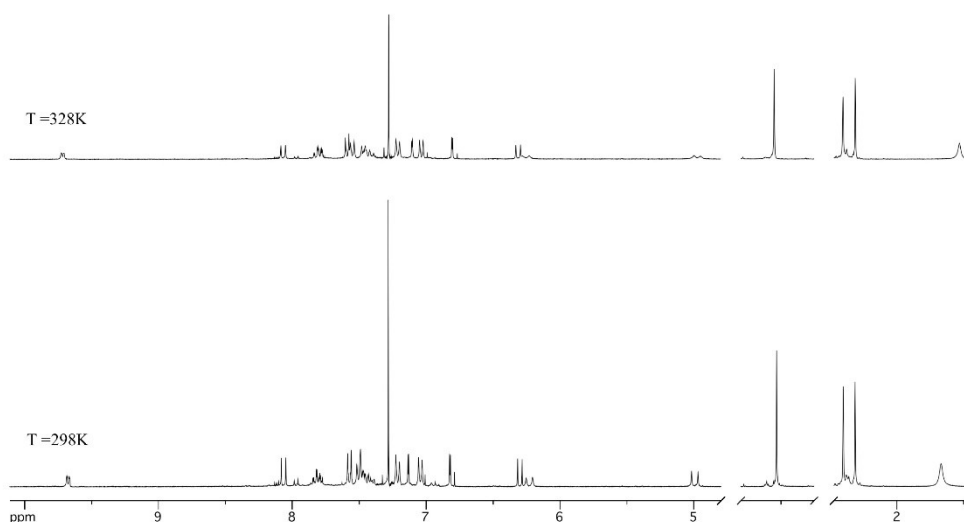


**Fig. S3a:**  $^1\text{H}$  NMR spectra of complex **1c** in  $\text{CDCl}_3$ , recorded at 298 K and at 328 K. At this last temperature the spectrum remains unaltered even after 24 hours. The broadening of some signals is ascribable to dynamic processes activated at high temperature (ring inversion of chelating ligand).

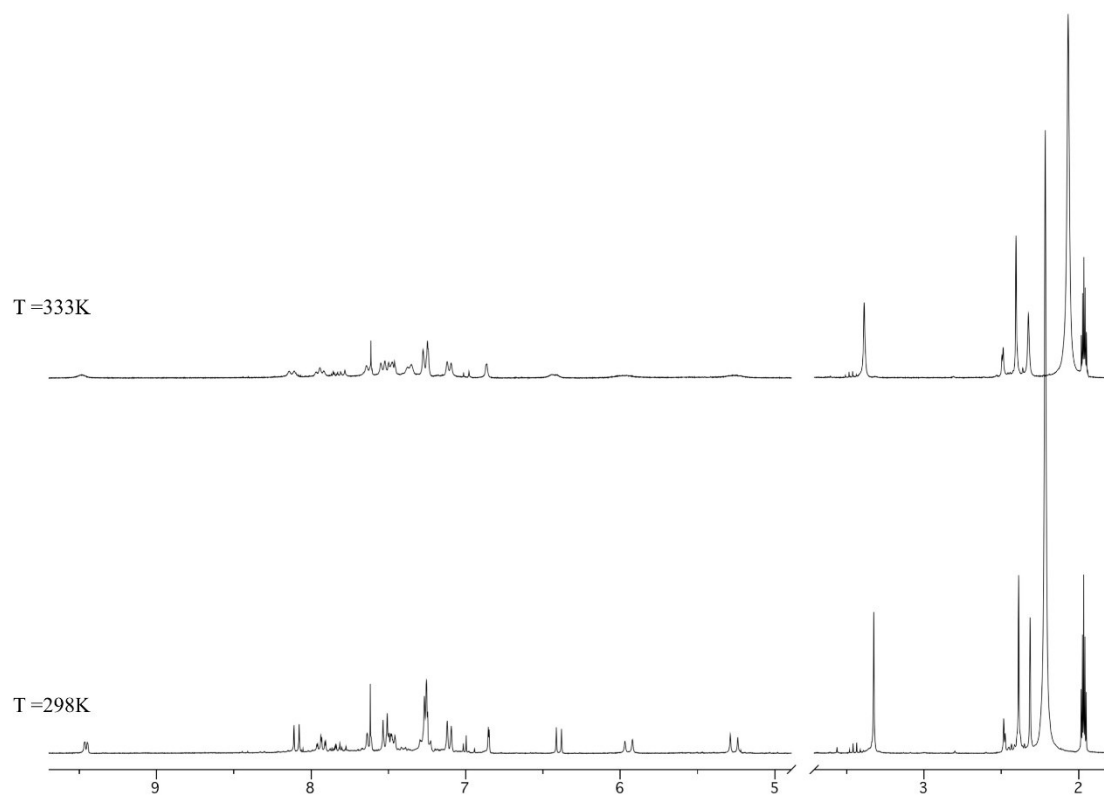


**Fig. S3b:** <sup>1</sup>H NMR spectra of complex **1c** in CD<sub>3</sub>CN, recorded at 298 K and at 333 K. At this last temperature the spectrum remains unaltered even after 24 hours. The broadening of some signals is ascribable to dynamic processes activated at high temperature (ring inversion of chelating ligand).

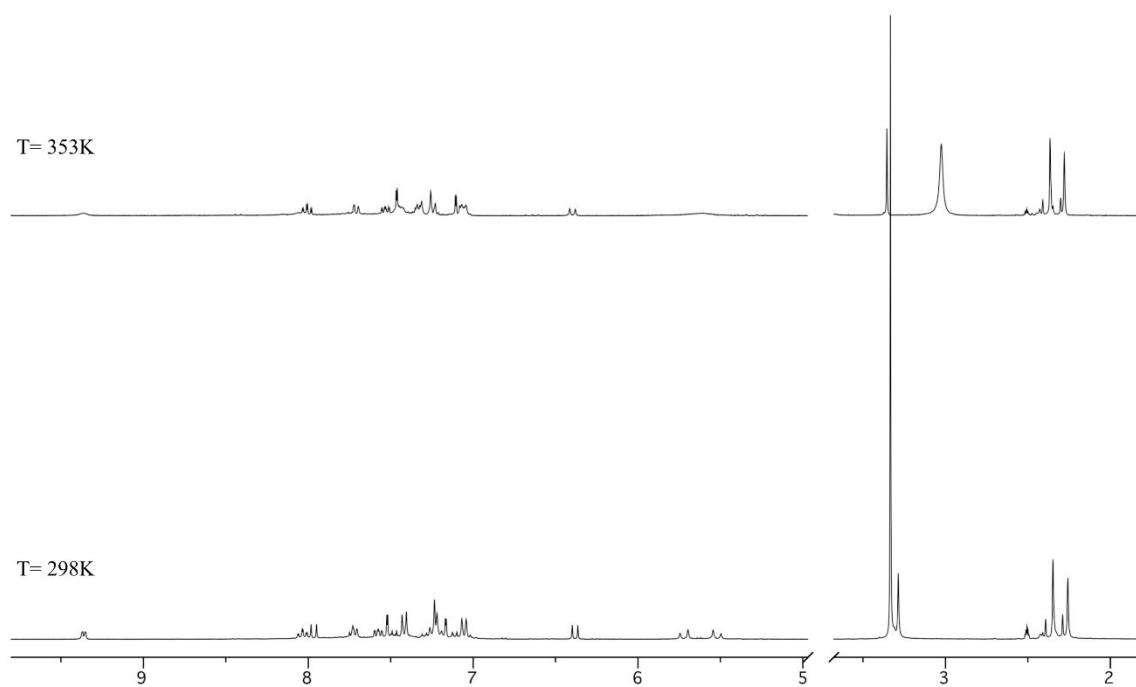


**Fig. S3c:**  $^1\text{H}$  NMR spectra of complex **1c** in  $\text{dms}\text{-d}_6$ , recorded at 298 K and at 353 K. At this last temperature the spectrum remains unaltered even after 24 hours. The broadening of some signals is ascribable to dynamic processes activated at high temperature (ring inversion of chelating ligand).

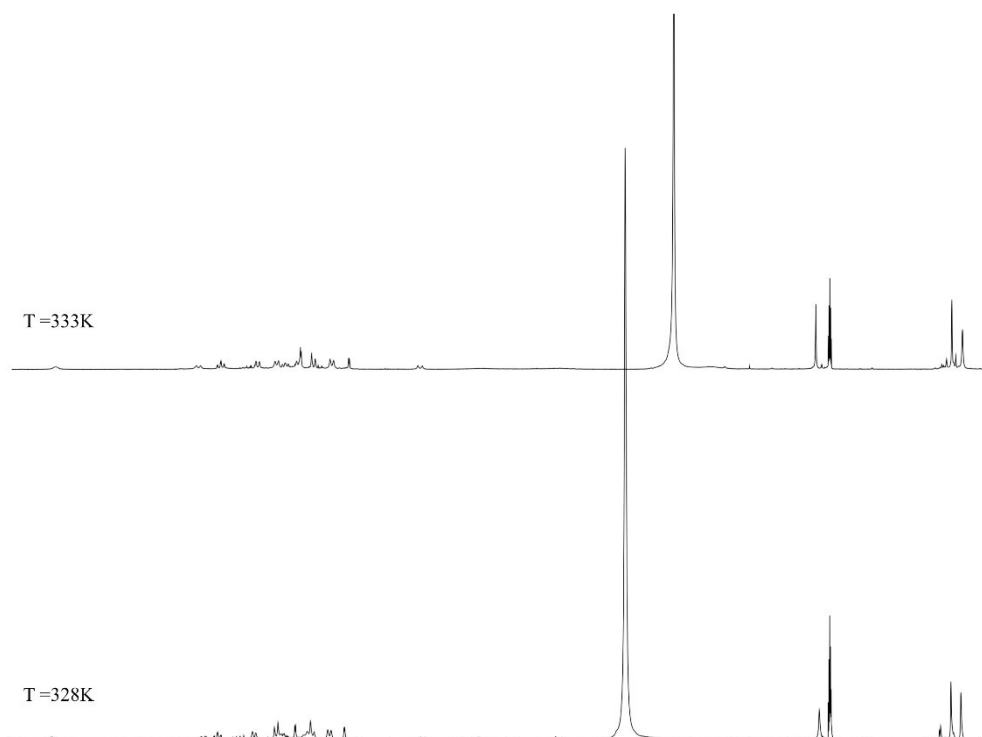


**Fig. S3d:**  $^1\text{H}$  NMR spectra of complex **1c** in  $\text{CD}_3\text{OD}$ , recorded at 298 K and at 333 K. At this last temperature the spectrum remains unaltered even after 24 hours. The broadening of some signals is ascribable to dynamic processes activated at high temperature (ring inversion of chelating ligand)

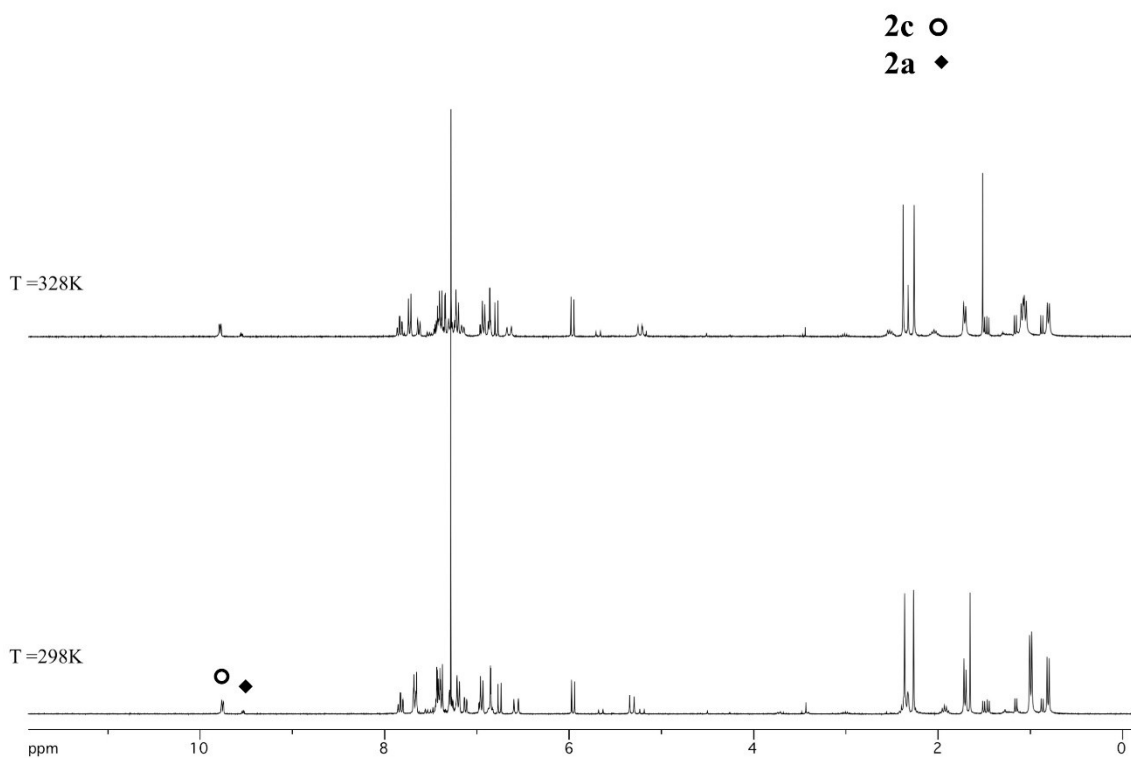


**Fig. S3e:**  $^1\text{H}$  NMR spectra of final mixture of **2a/2c** in  $\text{CDCl}_3$ , recorded at 298 K and 328 K. At this last temperature the solution was kept for 24h without changing its composition.

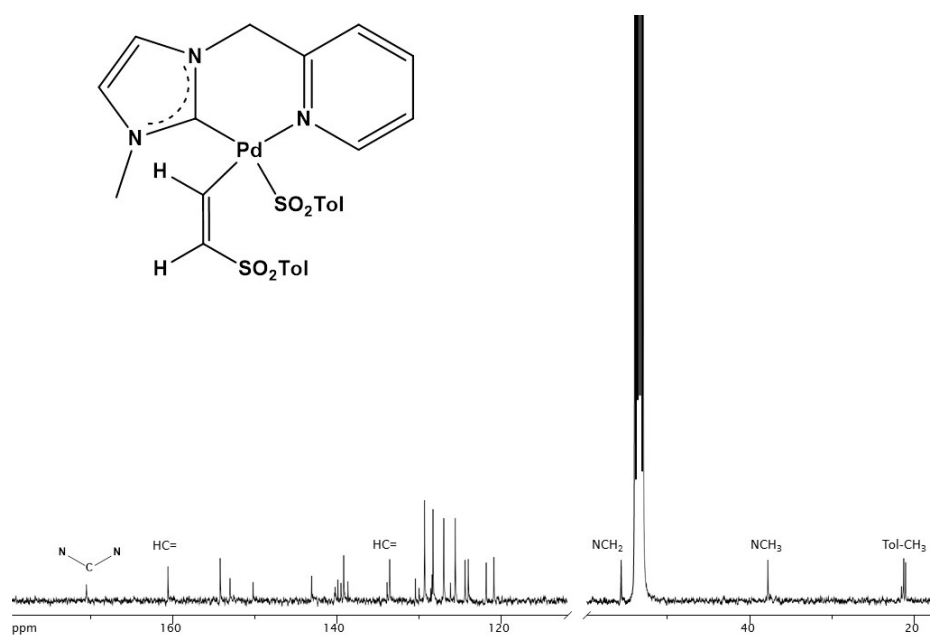


**Fig. S4a:**  $^{13}\text{C}$   $\{^1\text{H}\}$  NMR spectrum of complex **1c** in  $\text{CD}_2\text{Cl}_2$  at 298 K

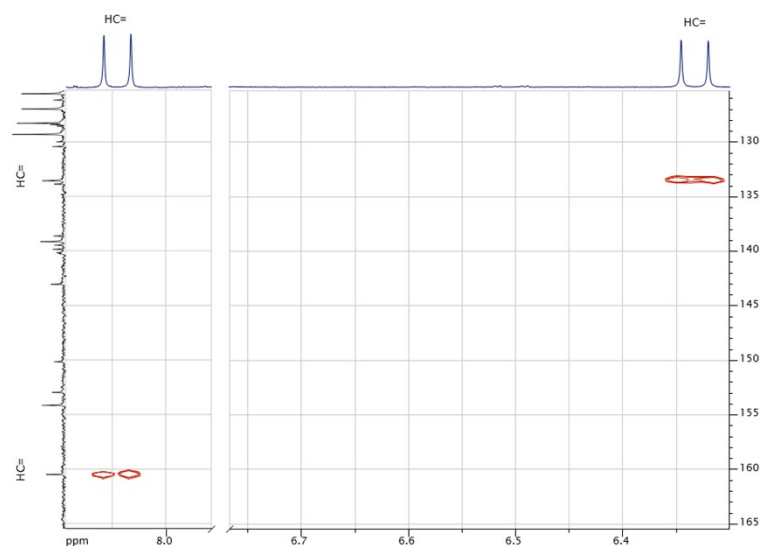


**Fig. S4b:** Selected part of the HSQC spectrum of the complex **1c** recorded at 233 K in  $\text{CD}_2\text{Cl}_2$  identifying the vinyl carbons

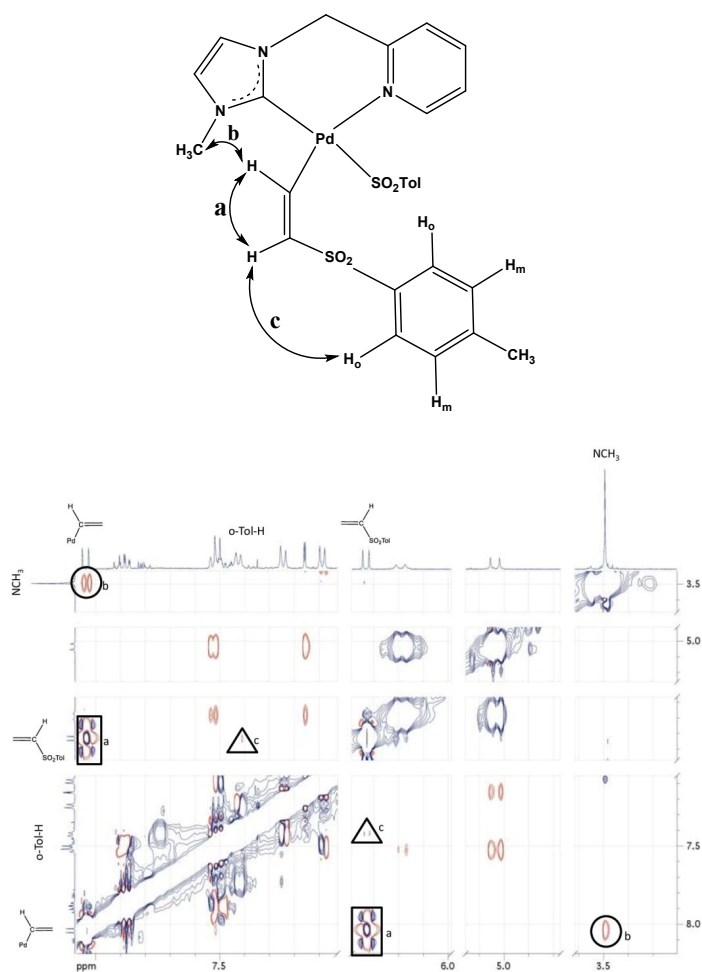


**Fig. S4c:** NOE interactions (up) and selected part of the NOESY spectrum of the complex **1c** in  $\text{CD}_2\text{Cl}_2$  at 233 K (down)

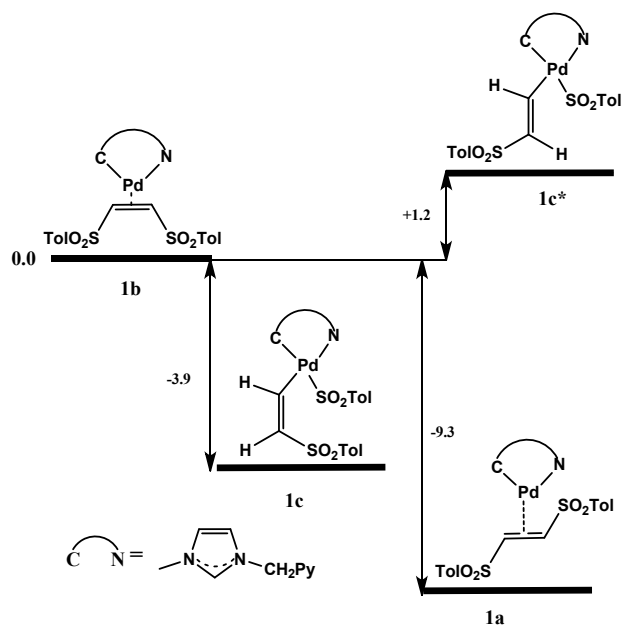


**Fig. S5:** Graphic representation of the DFT computational output.

**Table S1.** Crystallographic data.

Compound	2c
Formula	$\text{PdC}_{37}\text{H}_{41}\text{N}_3\text{O}_4\text{S}_2$
$M/\text{g}\cdot\text{mol}^{-1}$	762.25
Space group	$P 2_1/c$
Crystal system	Monoclinic
$a/\text{\AA}$	15.158(3)
$b/\text{\AA}$	11.271(2)
$c/\text{\AA}$	20.489(4)
$\alpha/^\circ$	90
$\beta/^\circ$	95.62(3)
$\gamma/^\circ$	90
$V/\text{\AA}^3$	3483.7(12)
$Z$	4
T/K	100(2)
$D_c/\text{g}\cdot\text{cm}^{-3}$	1.453
$F(000)$	1576
$\mu/\text{mm}^{-1}$	0.660
Measured Reflections	47816
Unique Reflections	11174
$R_{\text{int}}$	0.0298
Obs. Refl.ns [ $I \geq 2\sigma(I)$ ]	8912
$\theta_{\text{min}} - \theta_{\text{max}}/^\circ$	1.33 – 30.96

hkl ranges	-21,22; -15,15; -30,30
R(F <sup>2</sup> ) (Obs.Refl.ns)	0.0369
wR(F <sup>2</sup> ) (All Refl.ns)	0.1023
No. Variables	430
Goodness of fit	1.021
$\Delta\rho_{\max}; \Delta\rho_{\min} / e \cdot \text{\AA}^{-3}$	1.92; -1.10
CCDC Deposition N.	1970548

**Table S2.** Selected palladium coordination spheres distances and angles ( $\text{\AA}$  and degrees) for **2c** (grey sticks) and the bromo[3-(2,6-diisopropylphenyl)-1-( $\alpha$ -lutidyl)imidazol-2-ylidene]methyl-palladium(II) complex CCDC 194155.

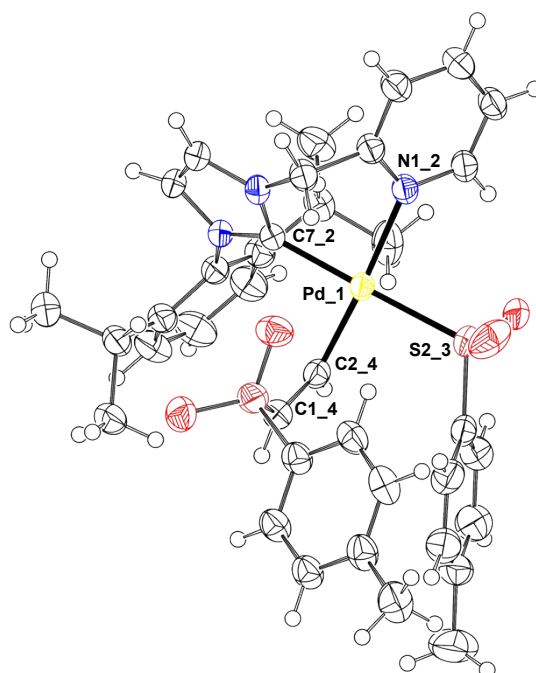
<b>2c (100 K)</b>				<b>CCDC 194155 (150 K)</b>			
Distances	( $\text{\AA}$ )	Angles	( $^\circ$ )	Distances	( $\text{\AA}$ )	Angles	( $^\circ$ )
Pd_1-C7_2	2.014(2)	C7_2-Pd_1-N1_2	85.88(7)	Pd1-C2	1.970(4)	C2-Pd1-N1	85.3(1)
Pd_1-N1_2	2.146(2)	S2_3-Pd_1-C2_4	91.21(6)	Pd1-N1	2.169(3)	Br1-Pd1-C1	89.97(7)
Pd_1-S2_3	2.314(1)	C7_2-Pd_1-C2_4	90.43(8)	Pd1-Br1	2.489(1)	C2-Pd1-C1	914(1)
Pd_1-C2_4	1.978(2)	N1_2-Pd_1-S2_3	92.46(5)	Pd1-C1	2.126(3)	N1-Pd1-Br1	93.33(8)
C2_4=C1_4	1.329(3)	Pd Ave.-C=C Plane <sup>b</sup>	75.67(5)	C=C	N.A.	Pd Ave.-C=C Plane <sup>b</sup>	N.A.
Pd-Ave. Coord. Plane <sup>a</sup>	0.021(1)	Pd Ave.-NHC Planes <sup>c</sup>	43.81(6)	Pd-Ave. Coord. Plane <sup>a</sup>	0.018(1)	Pd Ave.-NHC Planes <sup>c</sup>	44.45(10)

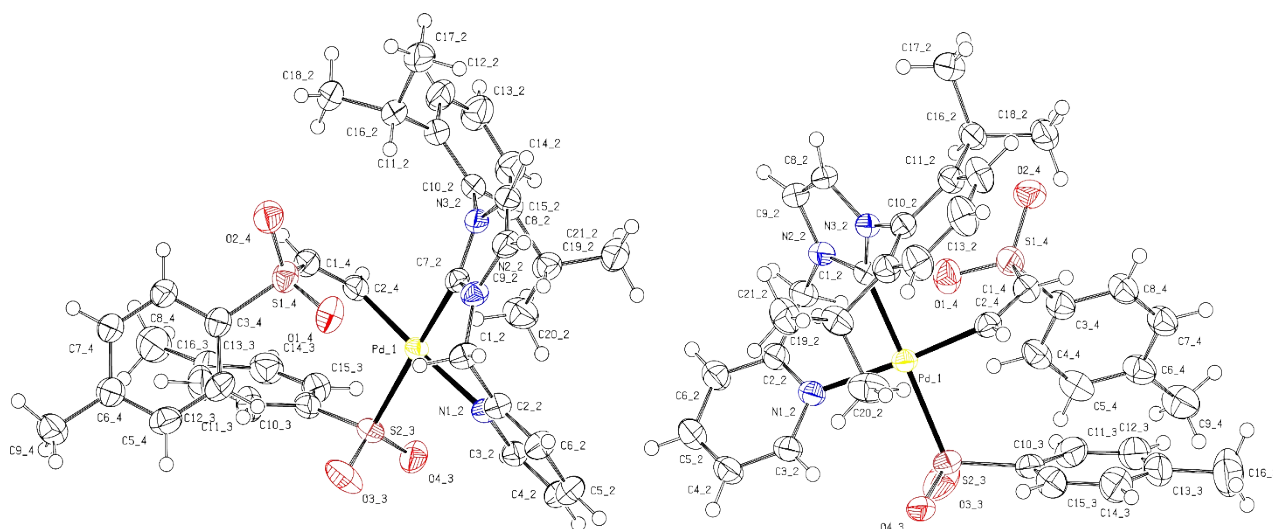
<sup>a</sup> Pd atom distance from the mean plane, calculated from the coordinates of the 4 atoms directly bound to the metal.

<sup>b</sup> Angle between the mean metal coordination plane and the olefin plane.

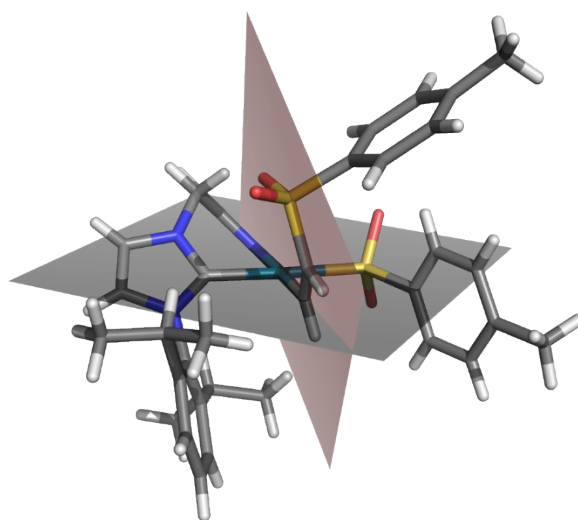
<sup>c</sup> Angle between the mean metal coordination plane and the NHC imidazole ring plane.

**Fig. S6.** Ortep representation of complex **2c** (ellipsoids dimensions correspond to 50% probability). Atom labels in use are reported.

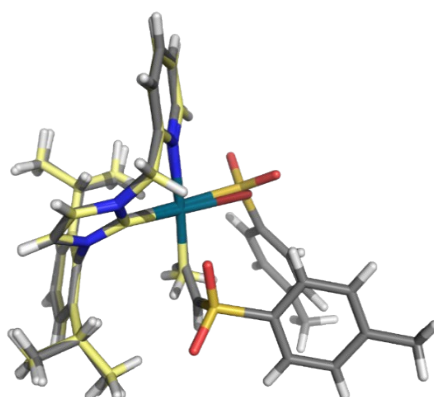




**Fig. S7.** Stick representation of **2c** showing the angle of  $75.67(5)^\circ$  between the Pd coordination plane and the vinyl ligand.



**Fig. S8.** Stick representation of **2c** (grey sticks) overlapped to CCDC 194155 (yellow sticks), showing the equivalent conformations adopted by the 1-( $\alpha$ -picolyl)imidazol-2-ylidene ligand (R.M.S.D. = 0.10 Å).



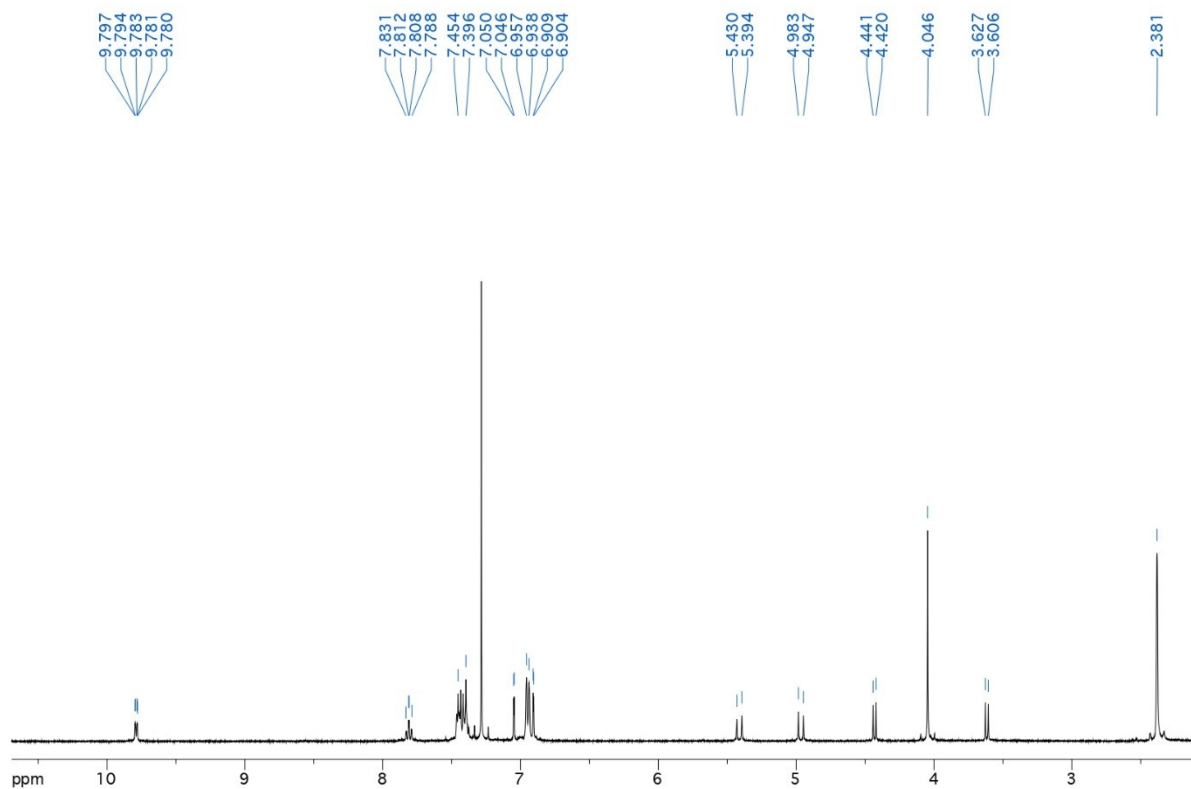


**Fig. S9:**  $^1\text{H}$  NMR spectrum of complex **1a** in  $\text{CDCl}_3$  at 298 K

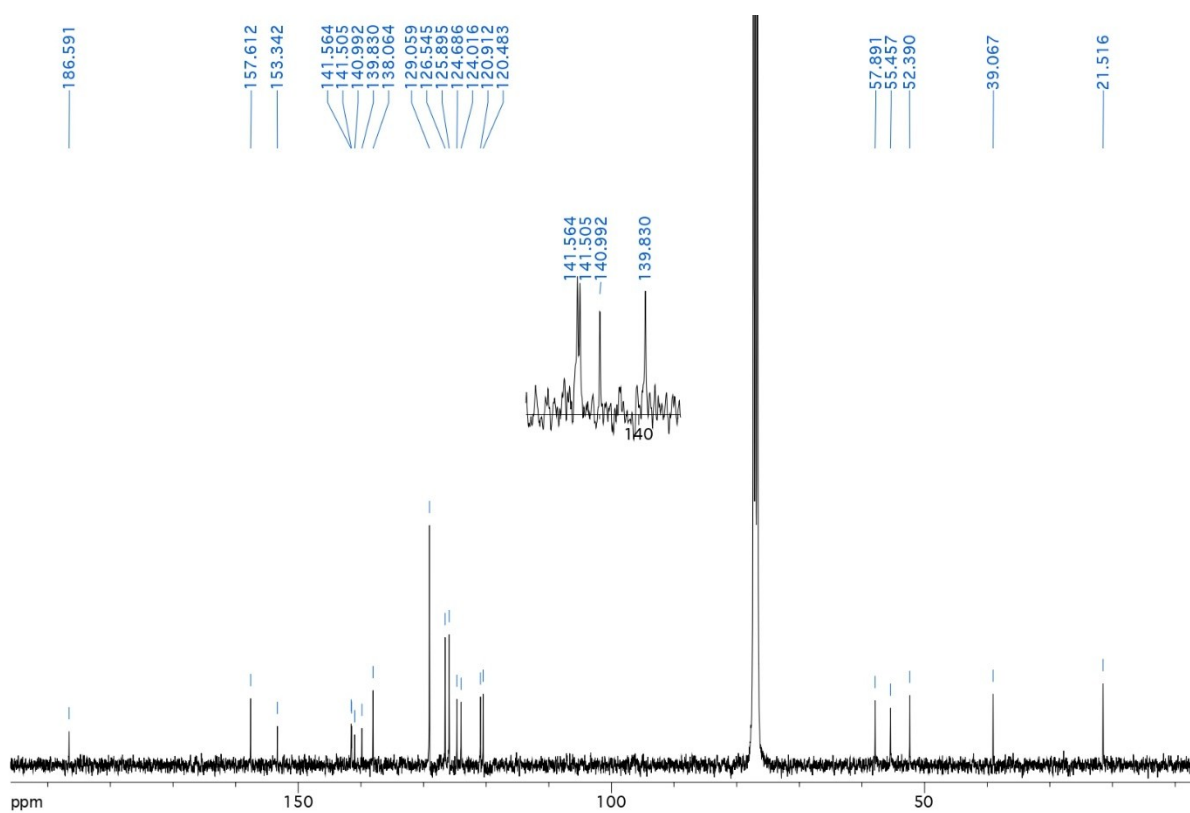


**Fig. S10:**  $^{13}\text{C}\{^1\text{H}\}$  NMR spectrum of complex **1a** in  $\text{CDCl}_3$  at 298 K

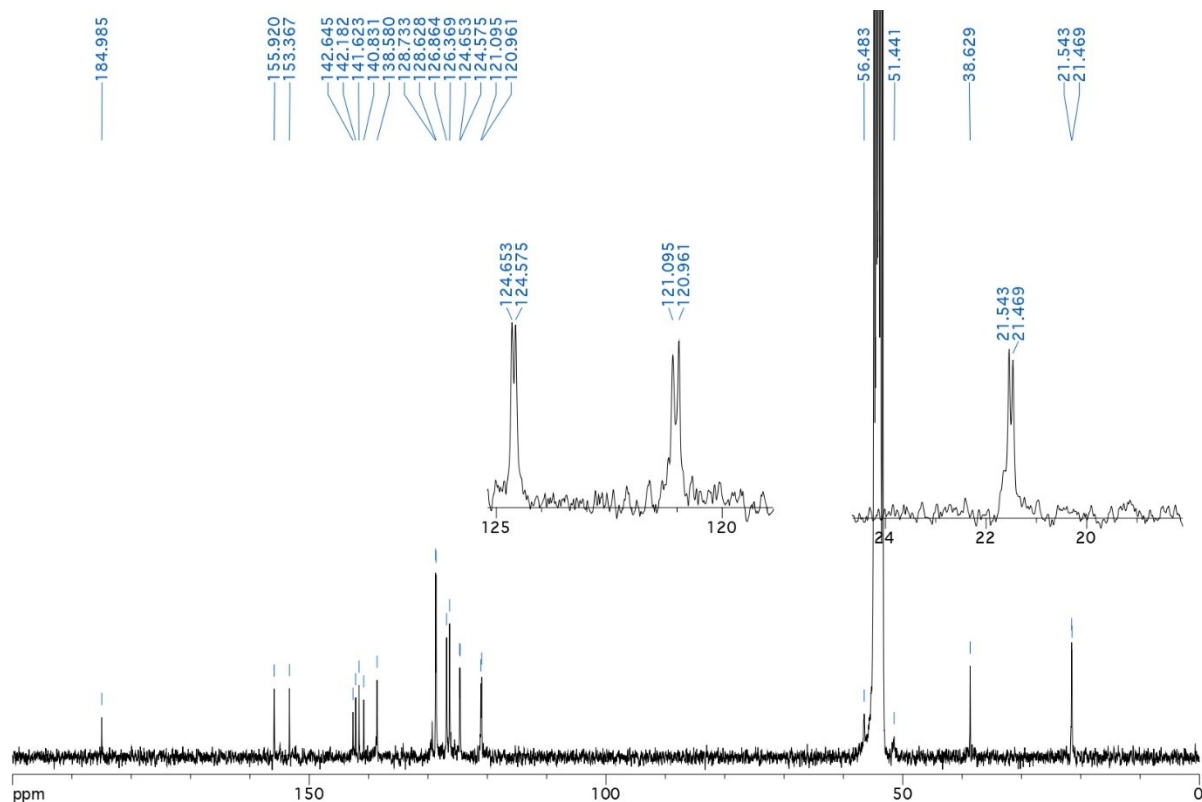


**Fig. S11:**  $^{13}\text{C}\{^1\text{H}\}$  NMR spectrum of complex **1b** in  $\text{CD}_2\text{Cl}_2$  at 233 K

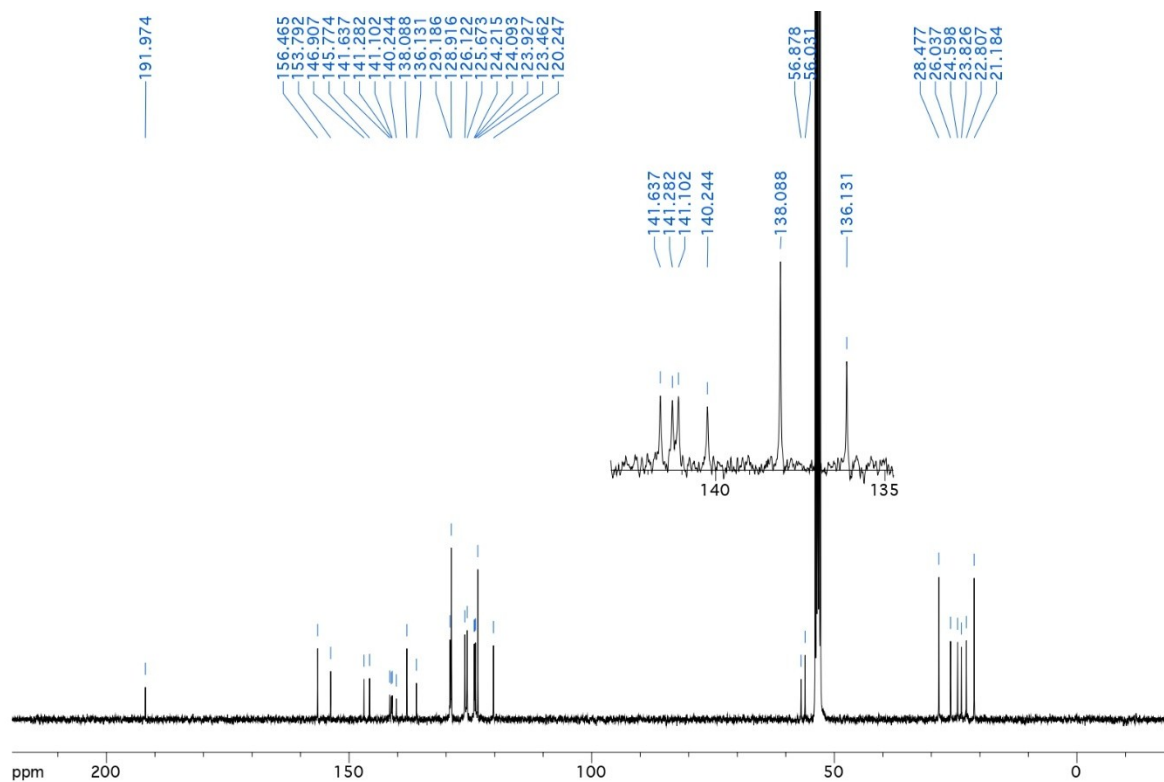


**Fig. S12:**  $^{13}\text{C}\{^1\text{H}\}$  NMR spectrum of complex **2a** in  $\text{CD}_2\text{Cl}_2$  at 298 K

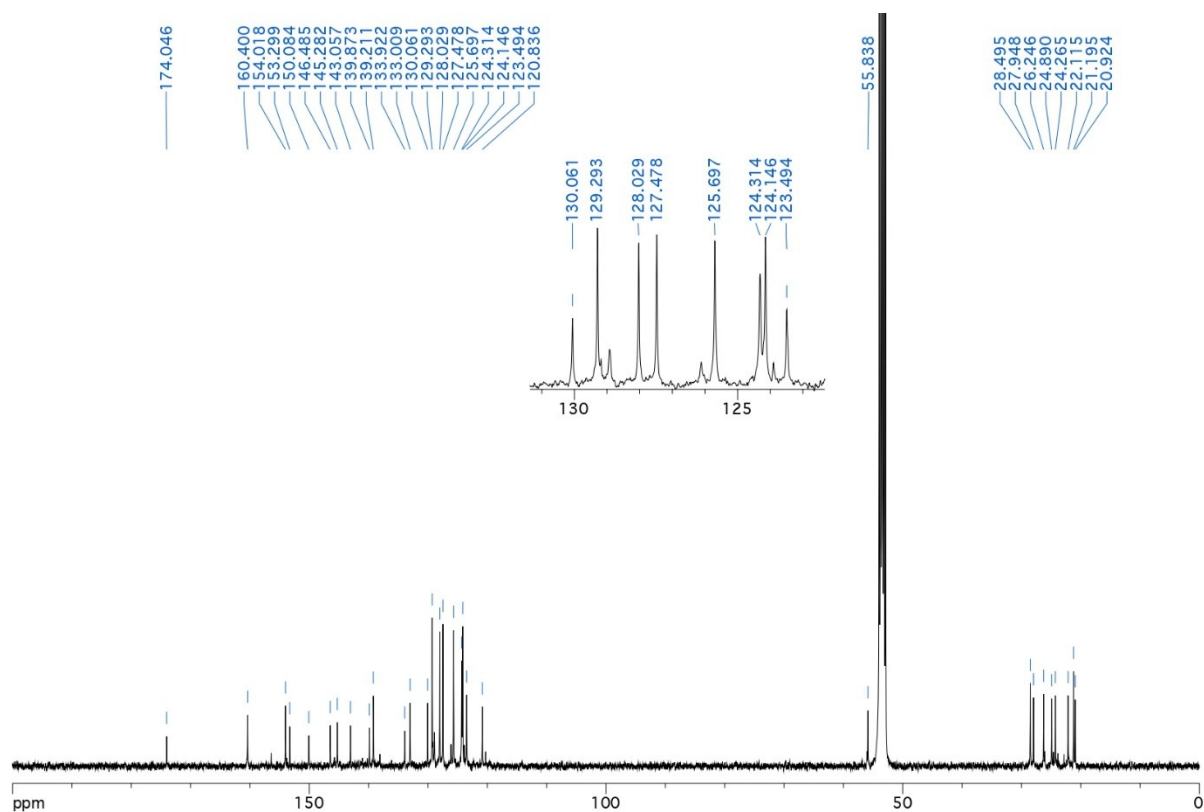


**Fig. S13:**  $^{13}\text{C}\{^1\text{H}\}$  NMR spectrum of final mixture of **2a/2c** in  $\text{CDCl}_3$  at 298 K

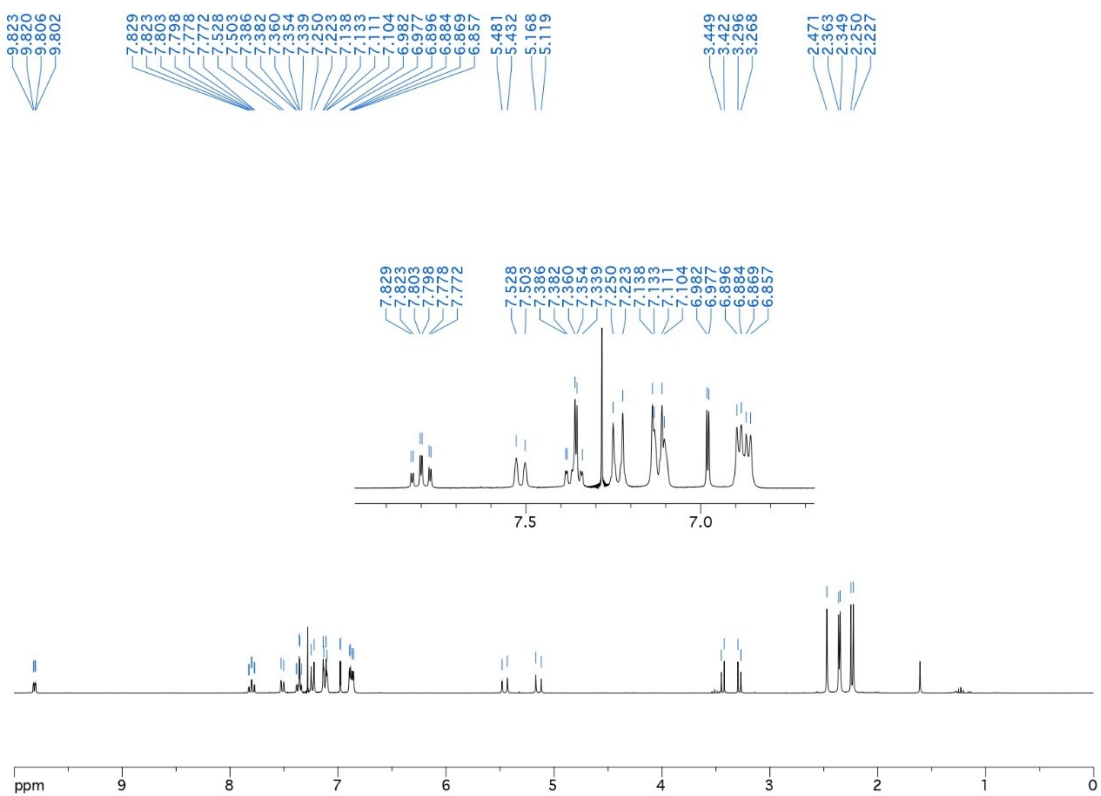


**Fig. S14:**  $^1\text{H}$  NMR spectrum of complex **3a** in  $\text{CDCl}_3$  at 298 K

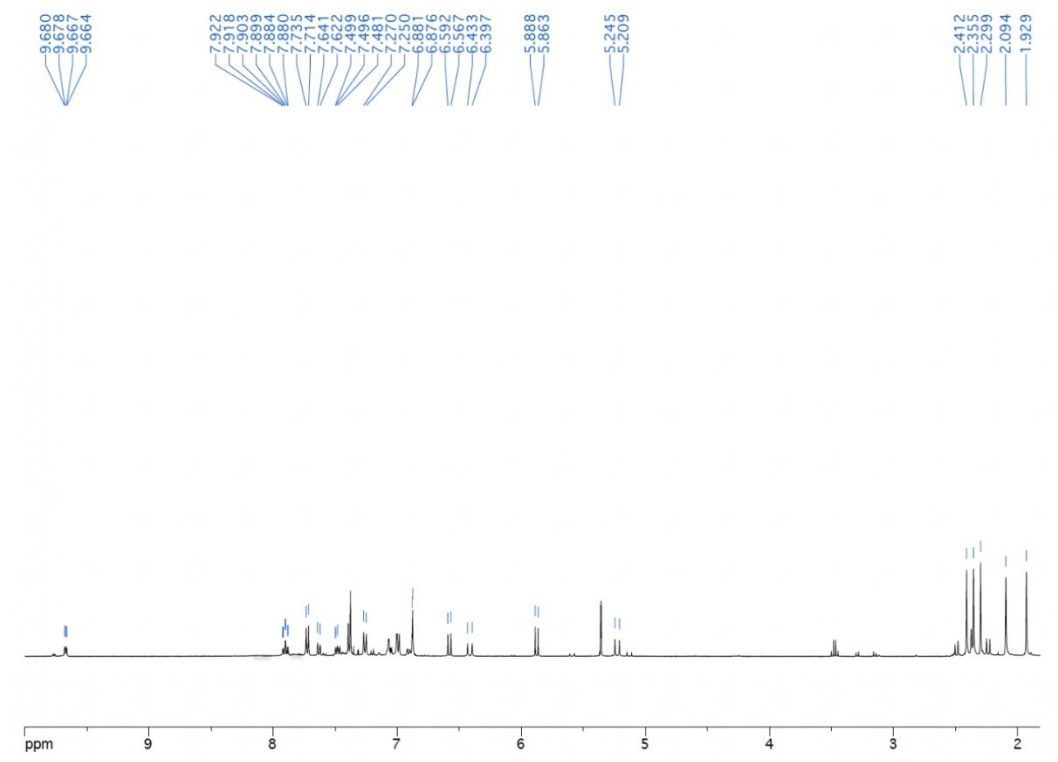


**Fig. S15:**  $^1\text{H}$  NMR spectrum of final mixture of **3a/3c** in  $\text{CD}_2\text{Cl}_2$  at 298 K

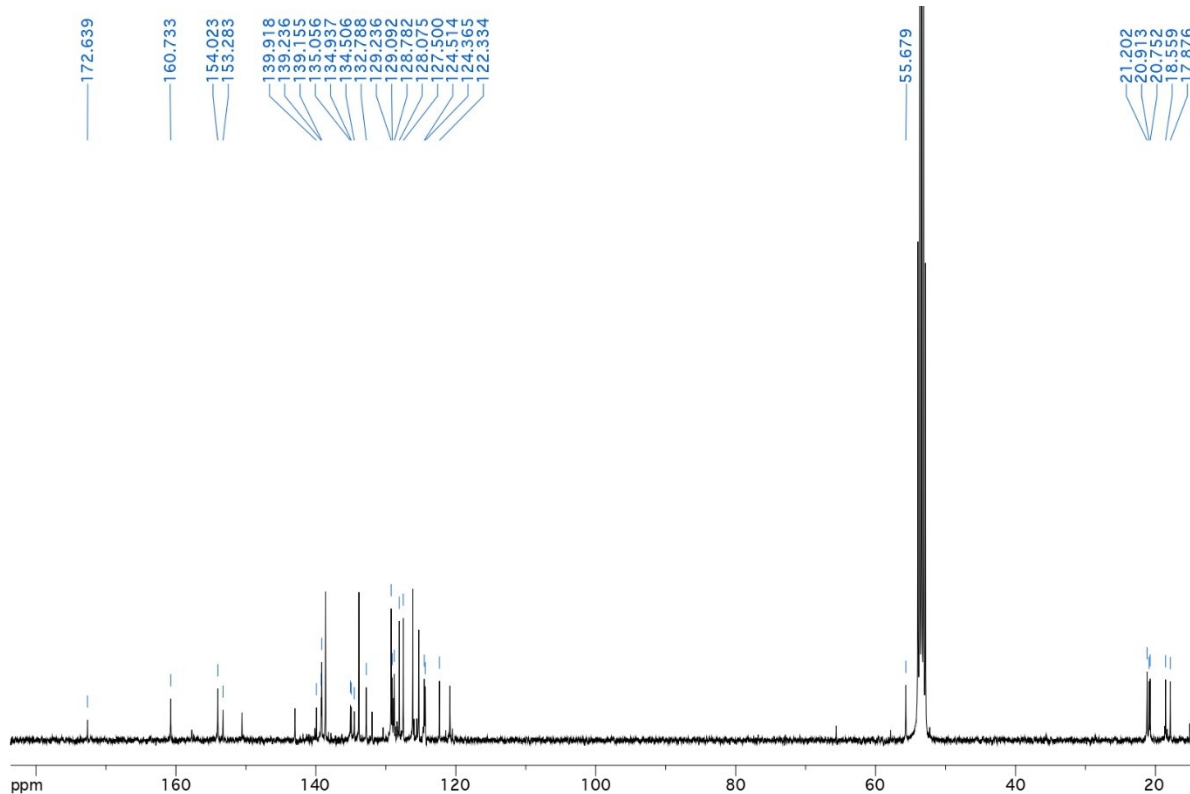


**Fig. S16:**  $^{13}\text{C}\{^1\text{H}\}$  NMR spectrum of final mixture of **3a/3c** in  $\text{CD}_2\text{Cl}_2$  at 298 K